



Original Article

High-temperature energy storage properties in polyimide-based nanocomposites filled with antiferroelectric nanoparticles



Kailun Zou^a, Zhenhao Fan^a, Chaohui He^a, Yinmei Lu^a, Haitao Huang^b,
Qingfeng Zhang^{a,*}, Yunbin He^{a,*}

^a Ministry of Education Key Laboratory of Green Preparation and Application for Functional Materials, Hubei Key Lab of Ferro & Piezoelectric Materials and Devices, Hubei Key Laboratory of Polymer Materials, School of Materials Science & Engineering, Hubei University, Wuhan 430062, China

^b Department of Applied Physics, The Hong Kong Polytechnic University, Hong Kong, China

ARTICLE INFO

Article history:

Received 24 June 2020

Accepted 7 August 2020

Available online 23 August 2020

Keywords:

Antiferroelectric

Nanocomposites

High temperature

Energy storage

Dielectric capacitors

ABSTRACT

Inorganic ferroelectric filler/polymer nanocomposites combining large maximum electric displacement (D_{\max}) of ferroelectric materials with good flexibility and high electric breakdown strength (E_b) of the polymers are regarded as the most promising materials for preparing flexible dielectric capacitors with superior energy storage properties. Besides dielectric capacitors are always faced with high temperature environment in many application cases, and thus the applicability of high temperature is also highly desired. To develop nanocomposite-based dielectric capacitors with superior energy storage properties in a wide temperature range, in this study, we synthesize $\text{Pb}_{0.97}\text{La}_{0.02}(\text{Zr}_{0.5}\text{Sn}_{0.38}\text{Ti}_{0.12})\text{O}_3$ (PLZST) antiferroelectric nanoparticles (NPs) with larger D_{\max} and smaller remnant electric displacement (D_r) in comparison with ferroelectric nanoparticles and disperse them into polyimide (PI) polymer matrix with good temperature stability. The results indicate that by adjusting reasonably the PLZST filler content, in a wide temperature range of 20–120 °C, 7 wt.% PLZST/PI nanocomposite exhibits slim electric displacement-electric field hysteresis loops and low D_r , and thus the discharge energy density and energy efficiency are always higher than 4 J/cm³ and 90%, respectively. These indicate this nanocomposite is a good candidate material for developing flexible dielectric capacitors applicable in high temperature environment.

© 2020 The Author(s). Published by Elsevier B.V. This is an open access article under the CC BY-NC-ND license (<http://creativecommons.org/licenses/by-nc-nd/4.0/>).

1. Introduction

In energy storage devices, dielectric capacitors have obvious advantages such as high power density (megawatt level),

fast charge and discharge speeds, high operating voltage and good safety in comparison with fuel cells, batteries, and electrochemical capacitors [1–3]. Therefore, they have wide application prospects in microelectronics, hybrid vehicles, power grids, and electromagnetic cannons, which require high pulse power density [4–7]. However, dielectric capacitors currently in use have low energy density and thus a large volume or mass of the device is needed in order to provide large enough total energy for practical applications, which is not

* Corresponding authors.

E-mails: zhangqingfeng@hubu.edu.cn (Q. Zhang),
ybhe@hubu.edu.cn (Y. He).

<https://doi.org/10.1016/j.jmrt.2020.08.030>

2238-7854/© 2020 The Author(s). Published by Elsevier B.V. This is an open access article under the CC BY-NC-ND license (<http://creativecommons.org/licenses/by-nc-nd/4.0/>).

conductive to lightweight and miniaturization of electronic and electrical power systems [8,9]. Based on this issue, it is urgent to develop dielectric materials with high energy density to improve energy storage properties of dielectric capacitors. For dielectric materials, the total energy storage density (W), the discharge energy density (W_d) and the energy efficiency (η) can be given by the following equations, respectively [10,11].

$$W = \int_0^{D_{\max}} EdD \quad (\text{upon charging}) \quad (1)$$

$$W_d = \int_{D_r}^{D_{\max}} EdD \quad (\text{upon discharging}) \quad (2)$$

$$\eta = \frac{W_d}{W} \times 100\% \quad (3)$$

where D , D_{\max} , D_r and E are respectively the electric displacement, maximum electric displacement, remnant displacement and the applied electric field. From above equations, it can be found that in order to obtain dielectric materials with good energy storage ability, large D_{\max} , small D_r and high electric breakdown strength (E_b) are necessary. Thus, recently, polymer-based nanocomposites by combining polymers with high E_b and ceramic materials with large D_{\max} have become a research hotspot in the field of dielectric energy storage.

For polymer materials, ferroelectric polymers, such as polyvinylidene fluoride (PVDF), polyvinylidene fluoride-hexafluoropropylene (PVDF-HFP), and poly(vinylidene fluoride-trifluoroethylene-chlorotrifluoroethylene) (PVDF-TrFE-CTFE), are commonly used, due to their large D_{\max} and good machinability [12–14]. However, these polymer materials have usually low glass-transition temperature (T_g) [15,16]. When the working environment temperature comes near to their T_g values, the D_{\max} will decrease sharply, which leads to low energy density. Therefore, ferroelectric polymer-based dielectric capacitors are not capable of being applied in some extreme environment such as hybrid electric vehicles, in which the working temperature is up to 150 °C [17]. In comparison with ferroelectric polymers, Polyimide (PI) has higher T_g (>360 °C) and thus possesses superior thermal stability [4]. What is more, its mechanical and electrical insulation performances are excellent. Based on these, PI is a promising candidate for preparing nanocomposite based high-temperature dielectric capacitors.

For nanofillers in polymer-based nanocomposites, ferroelectric materials with large D_{\max} , such as BaTiO₃ and Ba_xSr_{1-x}TiO₃ are usually adopted on the purpose of improving energy density [18,19]. However, their large D_r restricts the further improvement of the W_d and causes low η [20,21]. Compared with ferroelectrics, antiferroelectrics (AFE) possess much smaller D_r (near zero) and larger $D_{\max}-D_r$ values, and thus if they are used as the fillers of the nanocomposites, high W_d and η may be obtain simultaneously [2,5,9,22].

Based on above discussions, in this work, we develop and prepare Pb_{0.97}La_{0.02}(Zr_{0.5}Sn_{0.38}Ti_{0.12})O₃ (PLZST) AFE nanoparticles (NPs)/PI nanocomposites via a simple tape-casting method and investigate their energy storage properties. Benefited from excellent thermal stability of PI, and low D_r ,

high D_{\max} of Pb_{0.97}La_{0.02}(Zr_{0.5}Sn_{0.38}Ti_{0.12})O₃ AFE NPs, large W_d (>4J/cm³) and η (>90%) are achieved simultaneously in the nanocomposites over a wide temperature range of 20–120 °C.

2. Experimental procedures

The PLZST AFE NPs were synthesized by a sol-gel method, as reported in our previous work [9]. The PLZST/PI nanocomposite films were prepared via a tape-casting process. Firstly, 4, 4'-oxydianiline (ODA, 98%, Aladdin) was dissolved in N, N'-dimethyl-acetamide (DMAc, 99%, Sinopharm) and stirred for 1.5 h at the room temperature (RT) to form clear solution. Then, pyromellitic dianhydride (PMDA, 99%, Aladdin) was added to the above solution and stirred for 24 h to form poly(amic acid) (PAA) solution. After that, different contents of PLZST NPs (0, 1, 3, 5, 7, 10, 15, 20 wt.%) were added into the PAA solution and stirred vigorously for 24 h. The mixtures were quickly cast on clean glass substrates and then dried at 60 °C for 12 h in vacuum to completely remove the solvents. Subsequently, the nanocomposites were heated for thermal imidization at 100 °C for 30 min, 140 °C for 30 min, 180 °C for 1 h, 220 °C for 30 min and 250 °C for 2 h, respectively. Finally, the nanocomposite films with the thickness of ~20 μm were stripped from the glass substrate. Fig. 1 shows the schematic diagram for the formation process of the flexible PLZST NPs/PI nanocomposites. Aluminum electrodes with a diameter of 2.6 mm were deposited onto both sides of the nanocomposites through high-vacuum-resistance evaporation equipment (VZZ-300, VANNO, China) for electrical properties measurements.

The surface morphology and the element distribution were tested using a field-emission scanning electron microscopy (FE-SEM, SIGMA 500, Zeiss, Germany) equipped with an energy dispersive spectrometer (EDS, XFlash 6130, Bruker, Germany). The room-temperature dielectric properties were measured by a precision LCR meter (TH2827A, Tonghui Electronic Co., Ltd., China) at 100 kHz. The electric displacement versus electric field (D - E) hysteresis loops at different temperatures were acquired by a ferroelectric testing system (Precision LC II, Radiant Technologies Inc., USA) combined with a high-voltage amplifier (Trek 609B, Trek, USA) at 100 Hz.

3. Results and discussion

The surface morphology of PLZST AFE NPs/PI nanocomposites loaded with various PLZST NPs contents are shown in Fig. 2. As seen, the pure PI film is very dense and when the PLZST NPs content is lower (Fig. 2(b, c, e, f)), the NPs can be evenly distributed in the PI polymer matrix and this is also confirmed by the EDS element mapping images of the nanocomposites with 3 wt.% PLZST NPs (Fig. 2(d)), which is conducive to obtaining large E_b and thus high W_d . However, when the NPs content exceeds 7 wt.%, as given in Fig. 2(g)-(i), the surface of the film is not flat and some large particles are observed. This is mainly because at high filler content, the PLZST NPs begin to agglomerate in the polymer matrix due to their large surface energy, causing the formation of large particles. Besides, a large quantity of NPs fillers will cause the

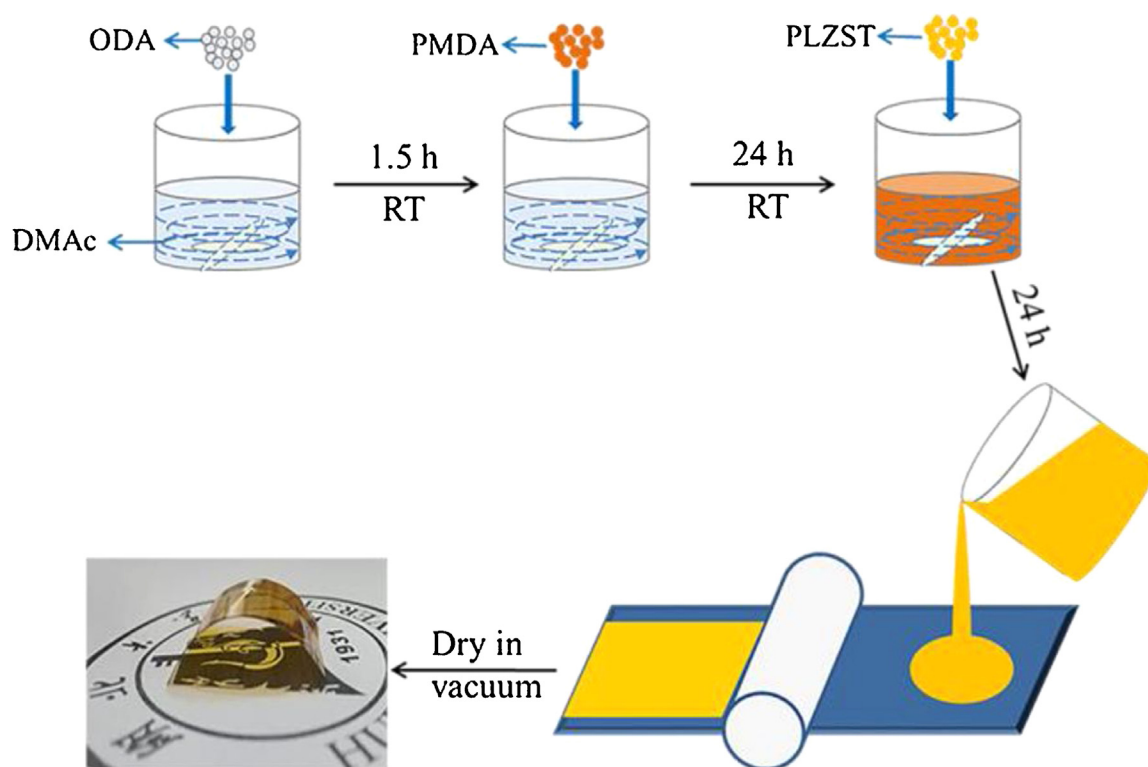


Fig. 1 – Schematic illustration of the formation process of PLZST/PI nanocomposites.

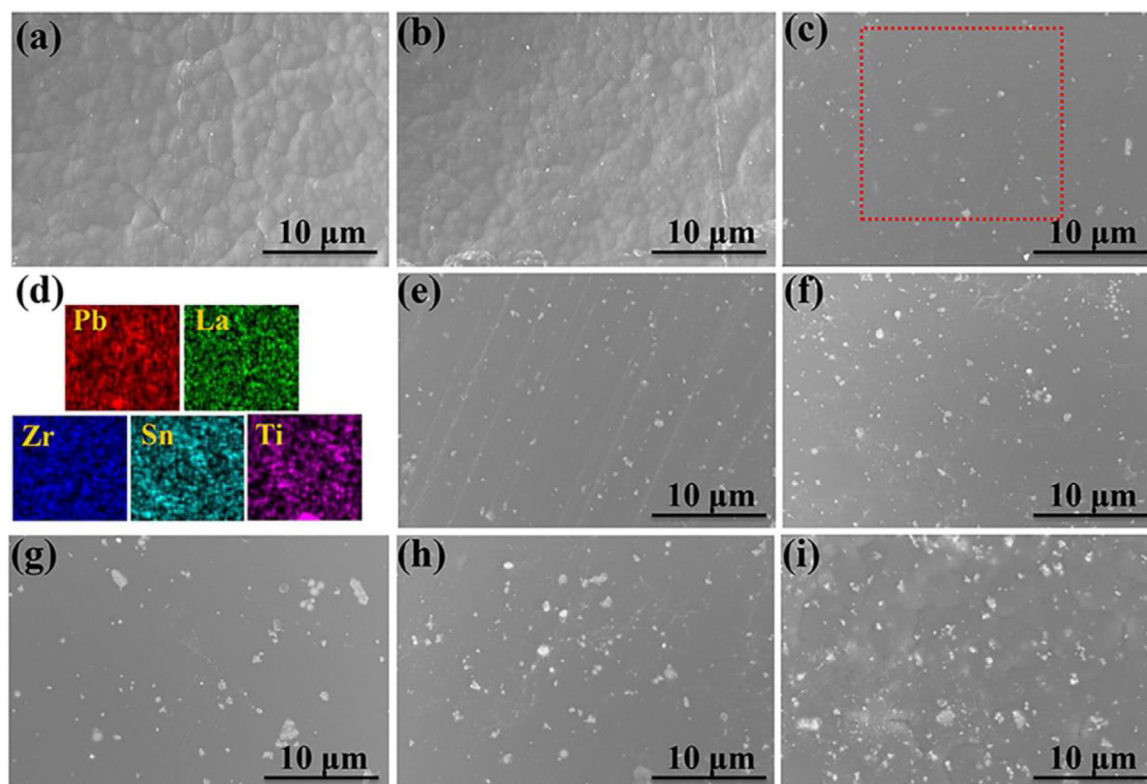


Fig. 2 – Surface FESEM images of PLZST/PI nanocomposites containing (a) 0 wt.%, (b) 1 wt.%, (c) 3 wt.%, (e) 5 wt.%, (f) 7 wt.%, (g) 10 wt.%, (h) 15 wt.% and (i) 20 wt.% NPs. (d) FESEM-EDS elemental mapping of the nanocomposites containing 3 wt.% NPs recorded at the square area marked by the red dashed lines.

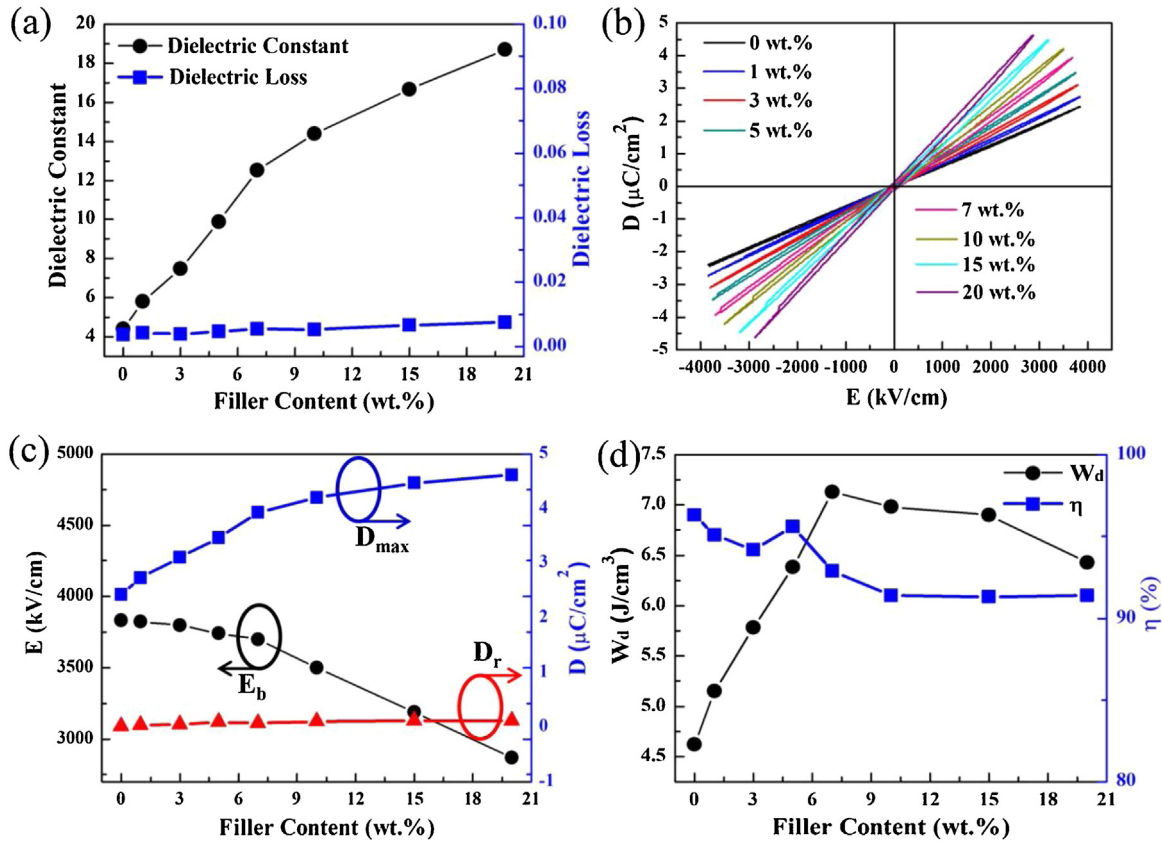


Fig. 3 – (a) Dielectric constant and dielectric loss, (b) room-temperature D - E loops, (c) D_{max} , D_r and E_b , and (d) W_d and η of PLZST/PI nanocomposites with different NPs contents.

introduction of more air and thus lead to the appearance of defects including voids and cracks during the vacuum drying process.

Fig. 3(a) and (b) displays the dielectric constant and loss, and D - E loops of PLZST/PI nanocomposites loaded with different PLZST NPs contents at the room temperature, respectively. Based on the D - E loops, we obtain the evolution of the D_{max} , D_r , E_b , W_d , and η of all nanocomposites, as given in Fig. 3(c) and (d). With increasing PLZST NPs contents, the dielectric constant of the nanocomposites obviously improves, which is mainly attributed to larger dielectric constant of the PLZST NPs compared with that of the PI polymer, and the Maxwell-Wagner-Sillars (MWS) interfacial polarization effect [9,23]. Moreover, the dielectric loss of all PLZST/PI nanocomposites is lower than 0.01, resulting from the very small dielectric loss of PLZST NPs and the PI polymer. The improved dielectric constant and the limited dielectric loss are beneficial for obtaining large W_d as well as high η in the nanocomposites. Besides, as displayed in Fig. 3(b), all nanocomposites display very slim D - E loops, and fairly low D_r values due to the small remnant electric displacement and electric hysteresis of AFE nanofillers themselves. With increasing the filler contents from 0 to 20 wt.%, the D_{max} value gradually rises from 2.43 to 4.62 $\mu\text{C}/\text{cm}^2$ due to larger D_{max} of PLZST in comparison with that of the pure PI and all D_r values are smaller than 0.05 $\mu\text{C}/\text{cm}^2$. When the filler content is lower than 10 wt.%, the E_b value slightly decreases from 3832 kV/cm for pure PI film

to 3700 kV/cm for 7 wt.% PLZST/PI film. However, with continuously increasing the fillers content, the E_b value sharply decreases to 2870 kV/cm. This is because at high filler content, the NPs begin to agglomerate in the polymer matrix due to their large surface energy, as seen in Fig. 2(g)-(i), which will give rise to an inhomogeneous local electric field in the nanocomposites, especially at interfaces between the fillers and polymer [24]. Due to high E_b of 3700 kV/cm and large D_{max} - D_r value of 3.86 $\mu\text{C}/\text{cm}^2$, the 7 wt.% PLZST/PI nanocomposite exhibits the most superior room-temperature energy storage properties with simultaneously large W_d of 7.13 J/cm^3 and high η of 92.9%.

Fig. 4(a)-(c) displays D - E loops, E_b , D_{max} , D_r values, and energy storage properties of the nanocomposite with 7 wt.% PLZST NPs contents in the temperature range of 20–120 °C, respectively. It can be obviously found that from 20 to 120 °C, the E_b decreases from 3700 to 2829 kV/cm due to the thermal breakdown, and the D_{max} declines from 3.93 to 2.93 $\mu\text{C}/\text{cm}^2$, but the D - E loops are still very slim and the D_r values are always small, which is attributed to superior thermal stability of PLZST materials and PI polymer [5,25]. As a result, in a wide temperature range of 20–120 °C, the W_d is always more than 4 J/cm^3 , and meanwhile the energy efficiency still maintains above 90%, which indicates 7 wt.% PLZST/PI nanocomposite is a promising material for applicable in high-temperature dielectric energy storage.

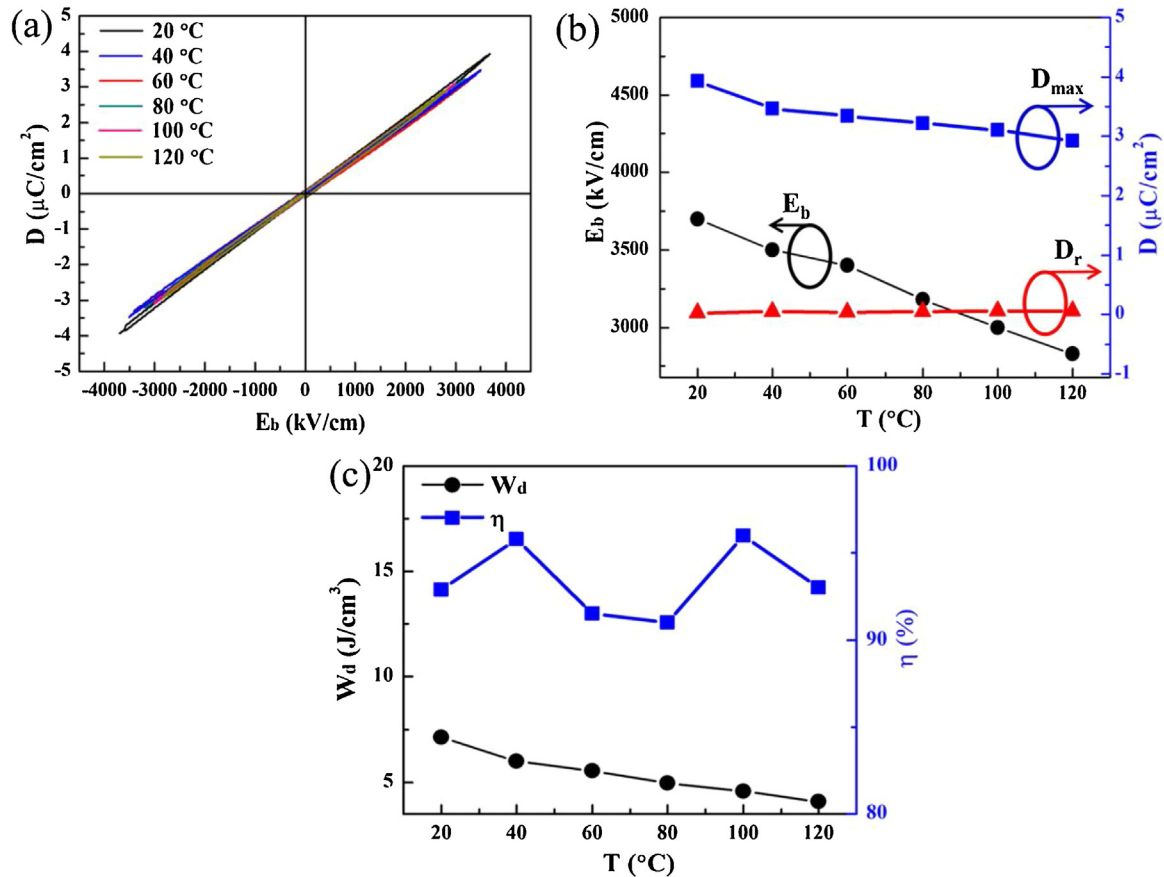


Fig. 4 – (a) D–E loops, (b) D_{\max} , D_r and E_b , and (c) W_d and η of 7 wt.% PLZST/PI nanocomposites in the temperature range of 20–120 °C.

Table 1 – Comparison of energy storage properties of polymer-based nanocomposites at the high temperature.

| Polymer matrix | Nanofillers | E_b (kV/cm) | W_d (J/cm ³) | η (%) | T (°C) | Ref. |
|----------------|----------------------------------|---------------|----------------------------|------------|--------|-----------|
| PC | None | 3000 | 0.8 | 70 | 150 | [4] |
| PEI | None | 4000 | 1.57 | 73.8 | 150 | |
| PI | BaTiO ₃ nanofibers | 5000 | 4.24 | ~50 | 100 | [25] |
| | | 4000 | 2.98 | ~60 | 150 | |
| | | 3500 | 1.74 | ~30 | 200 | |
| BOPP | None | 4200 | 2.1 | ~80 | 70 | [26] |
| | | 5000 | 6.0 | ~80 | 110 | |
| P(TFE-HFP) | None | 4100 | 2.5 | 80 | 130 | |
| | | 4800 | 3.5 | 97 | 70 | [27] |
| PI | BaTiO ₃ nanoparticles | 2750 | 1.3 | 40 | 100 | [28] |
| | | 2500 | 0.5 | 20 | 150 | |
| PI | PLZST nanoparticles | 3000 | 4.58 | 96 | 100 | This work |
| | | 2829 | 4.08 | 93 | 120 | |

Table 1 presents the comparison of the energy storage properties of recently reported polymer-based nanocomposites at the high temperature [4,25–28]. It is obviously seen that in comparison with other nanocomposites, 7 wt.% PLZST/PI nanocomposite obtained in this study exhibit simultaneously a larger W_d and higher η at the high temperature, indicating a good energy-storage temperature stability. This work provides a convenient, effective, and scalable way to developing and fabricating dielectric capacitors applicable in various temperature environments.

4. Conclusion

In conclusion, we successfully fabricate PLZST AFE NPs/PI nanocomposites with different NPs contents by tape-casting method and investigate their microstructure and energy storage properties. When the PLZST NPs content is lower than 10 wt.%, the NPs can be evenly distributed in PI polymer matrix, however, with the further increase, they begin to aggregate due to the high surface energy, resulting in the sharp reduction of the breakdown strength. With increas-

ing NPs contents from 0 to 20 wt.%, the dielectric constant of the nanocomposites improves from 4.4 to 18.7 and the D_{\max} rises from 2.43 to 4.62 $\mu\text{C}/\text{cm}^2$, which are due to larger dielectric constant and D_{\max} of PLZST AFE NPs as compared with the pure PI, and meanwhile the dielectric loss always maintains at a fairly low level (<0.01). By reasonably adjusting the PLZST content, 7 wt.% PLZST/PI nanocomposite exhibits a large ($D_{\max}-D_r$) of 3.93 $\mu\text{C}/\text{cm}^2$, a fairly small D_r of 0.07 $\mu\text{C}/\text{cm}^2$, and a high E_b of 3700 kV/cm and thus large discharge energy density of 7.13 J/cm³ and high energy efficiency of 92.9%. Furthermore, it is found that with increasing measuring temperature from 20 to 120 °C, the $D_{\max}-D_r$ value of the nanocomposite decreases slightly from 3.86 to 2.873 $\mu\text{C}/\text{cm}^2$, the D_r value is always lower than 0.1 $\mu\text{C}/\text{cm}^2$, and thus the discharge energy density and energy efficiency are larger than 4 J/cm³ and 90%, respectively. This work provides a new way for developing dielectric capacitors useful in high temperature environment.

Conflicts of interest

The authors declare no conflicts of interest.

Acknowledgements

This work was supported by the National Key R&D Program of China (Grant No. 2019YFB1503500), the National Natural Science Foundation of China (Grant Nos. 11774082, 51602093, 51872079, 11975093), the Natural Science Foundation of Hubei Province (Grant Nos. 2018CFB700, 2019CFA006, 2019CFA055), the Program for Science and Technology Innovation Team in Colleges of Hubei Province (T201901), Wuhan Application Foundation Frontier Project (No. 2018010401011287), Shenzhen Science, Technology and Innovation Commission (SGDX2019081623240364), and the Research Grants Council of the Hong Kong Special Administrative Region, China (Project No. PolyU152665/16E).

REFERENCES

- [1] Zhang X, Shen Y, Zhang QH, Gu L, Hu YH, Du JW, et al. Ultrahigh energy density of polymer nanocomposites containing BaTiO₃@TiO₂ nanofibers by atomic-scale interface engineering. *Adv Mater* 2015;27:819–24.
- [2] Zhang QF, Tong HF, Chen J, Lu YM, Yang TQ, Yao X, et al. High recoverable energy density over a wide temperature range in Sr modified (Pb,La) (Zr,Sn,Ti)O₃ antiferroelectric ceramics with an orthorhombic phase. *Appl Phys Lett* 2016;109:262901–11.
- [3] Liu B, Yang MH, Zhou WY, Cai HW, Zhong SL, Zheng MS, et al. High energy density and discharge efficiency polypropylene nanocomposites for potential high-power capacitor. *Energy Storage Mater* 2020;27:443–52.
- [4] Li Q, Chen L, Gadinski MR, Zhang SH, Zhang GZ, Li HU, et al. Flexible high-temperature dielectric materials from polymer nanocomposites. *Nature* 2015;523:576–9.
- [5] Dan Y, Xu HJ, Zou KL, Zhang QF, Lu YM, Chang G, et al. Energy storage characteristics of (Pb,La)(Zr,Sn,Ti)O₃ antiferroelectric ceramics with high Sn content. *Appl Phys Lett* 2018;113, 063902-1–5.
- [6] Zou KL, Dan Y, Xu HJ, Zhang QF, Lu YM, Huang HT, et al. Recent advances in lead-free dielectric materials for energy storage. *Mater Res Bull* 2019;113:190–201.
- [7] Liu G, Zhang TD, Feng Y, Zhang YQ, Zhang CH, Zhang Y, et al. Sandwich-structured polymers with electrospun boron nitrides layers as high-temperature energy storage dielectrics. *Chem Eng J* 2020;389:124443.
- [8] Jiang JY, Shen ZH, Cai XK, Qian JF, Dan ZK, Lin YH, et al. Polymer nanocomposites with interpenetrating gradient structure exhibiting ultrahigh discharge efficiency and energy density. *Adv Energy Mater* 2019;9: 1803411.
- [9] Zou KL, Dan Y, Yu YX, Zhang Y, Zhang QF, Lu YM, et al. Flexible dielectric nanocomposites with simultaneously large discharge energy density and high energy efficiency utilizing (Pb,La)(Zr,Sn,Ti)O₃ antiferroelectric nanoparticles as fillers. *J Mater Chem A* 2019;7:13473–82.
- [10] Chu BJ, Zhou X, Ren KL, Neese B, Lin MR, Wang Q, et al. A dielectric polymer with high electric energy density and fast discharge speed. *Science* 2006;313:334–6.
- [11] Zhang X, Shen Y, Xu B, Zhang QH, Gu L, Jiang JY, et al. Giant energy density and improved discharge efficiency of solution-processed polymer nanocomposites for dielectric energy storage. *Adv Mater* 2016;28:2055–61.
- [12] Qian K, Lv XG, Chen S, Luo H, Zhang D. Interfacial engineering tailoring the dielectric behavior and energy density of BaTiO₃/P(VDF-TrFE-CTFE) nanocomposites by regulating a liquid-crystalline polymer modifier structure. *Dalton Trans* 2018;47:12759–68.
- [13] Liu SH, Zhai JW. Improving the dielectric constant and energy density of poly(vinylidene fluoride) composites induced by surface-modified SrTiO₃ nanofibers by polyvinylpyrrolidone. *J Mater Chem A* 2015;3:1511–7.
- [14] Jiang JY, Shen ZH, Qian JF, Dan ZK, Guo MF, He Y, et al. Synergy of micro-/mesoscopic interfaces in multilayered polymer nanocomposites induces ultrahigh energy density for capacitive energy storage. *Nano Energy* 2019;62: 220–9.
- [15] Shaver AT, Yin K, Borjigin H, Zhang WR, Choudhury SR, Baer E, et al. Fluorinated poly(arylene ether ketone)s for high temperature dielectrics. *Polymer* 2016;83:199–204.
- [16] Zhang XM, Zhao YF, Wu YH, Zhang ZC. Poly(tetrafluoroethylene-hexafluoropropylene) films with high energy density and low loss for high-temperature pulse capacitors. *Polymer* 2017;114:311–8.
- [17] Johnson RW, Evans JL, Jacobsen P, Thompson JRR, Christopher M. The changing automotive environment: high-temperature electronics. *IEEE Trans Electron Packag Manuf* 2004;27:164–76.
- [18] Zhou L, Fu QY, Xue F, Tang XH, Zhou DX, Tian YH, et al. Multiple interfacial Fe₃O₄@BaTiO₃/P(VDF-HFP) core-shell-matrix films with internal barrier layer capacitor (IBLC) effects and high energy storage density. *ACS Appl Mater Interfaces* 2017;9:40792–800.
- [19] Liu SH, Xiu SM, Shen B, Zhai JW, Kong LB. Dielectric properties and energy storage densities of poly(vinylidene fluoride) nanocomposite with surface hydroxylated cube shaped Ba_{0.6}Sr_{0.4}TiO₃ nanoparticles. *Polymers* 2016;8:45.
- [20] Xie YC, Yu YY, Feng YF, Jiang WR, Zhang ZC. Fabrication of stretchable nanocomposites with high energy density and low loss from cross-linked PVDF filled with poly(dopamine) encapsulated BaTiO₃. *ACS Appl Mater Interfaces* 2017;9:2995–3005.
- [21] Hu PH, Song Y, Liu HY, Shen Y, Lin YH, Nan CW. Largely enhanced energy density in flexible P(VDF-TrFE) nanocomposites by surface-modified electrospun BaSrTiO₃ fibers. *J Mater Chem A* 2013;1:1688–93.

- [22] Zou KL, He CH, Yu YX, Huang J, Fan ZH, Lu YM, et al. Ultrahigh energy efficiency and large discharge energy density in flexible dielectric nanocomposites with $\text{Pb}_{0.97}\text{La}_{0.02}(\text{Zr}_{0.5}\text{Sn}_x\text{Ti}_{0.5-x})\text{O}_3$ antiferroelectric nanofillers. *ACS Appl Mater Interfaces* 2020;12:12847–56.
- [23] Han K, Li Q, Chen ZY, Gadinski MR, Dong LJ, Xiong CX, et al. Suppression of energy dissipation and enhancement of breakdown strength in ferroelectric polymer-graphene percolative composites. *J Mater Chem C* 2013;1:7034–42.
- [24] Kim P, Jones SC, Hotchkiss PJ, Haddock JN, Kippelen B, Marder SR, et al. Phosphonic acid-modified barium titanate polymer nanocomposites with high permittivity and dielectric strength. *Adv Mater* 2007;19:1001–5.
- [25] Hu PH, Sun WD, Fan MZ, Qian JF, Jiang JY, Dan ZK, et al. Large energy density at high-temperature and excellent thermal stability in polyimide nanocomposite contained with small loading of BaTiO_3 nanofibers. *Appl Surf Sci* 2018;458:743–50.
- [26] Zhang XM, Zhao YF, Wu YH, Zhang ZC. Poly(tetrafluoroethylene-hexa-fluoropropylene) films with high energy density and low loss for high-temperature pulse capacitors. *Polymer* 2017;114:311–8.
- [27] Liu FH, Li Q, Li ZY, Liu Y, Dong LJ, Xiong CX, et al. Poly(methylmethacrylate)/boron nitride nanocomposites with enhanced energy density as high temperature dielectrics. *Compos Sci Technol* 2017;142:139–44.
- [28] Sun W, Lu X, Jiang J, Zhang X, Hu P, Li M, et al. Dielectric and energy storage performances of polyimide/ BaTiO_3 nanocomposites at elevated temperatures. *J Appl Phys* 2017;121:244101.